The Canadian Mineralogist
Vol. 47, pp. 787-799 (2009)
DOI: 10.3749/canmin.47.4.787

GEOLOGY AND CHEMICAL VARIATIONS IN TOURMALINE FROM THE QUARTZ–TOURMALINE BRECCIAS WITHIN THE KERKENEZ GRANITE–MONZONITE MASSIF, CENTRAL ANATOLIAN CRYSTALLINE COMPLEX, TURKEY

SERHAT DEMİREL

Galata Energy, Resit Galip Cad. 111/54, G.O.P, TR–06700, Cankaya, Ankara, Turkey

M. CEMAL GÖNCÜOĞLU§

Middle East Technical University, Department of Geological Engineering, TR–06531, Ankara, Turkey

GÜLTEKIN TOPUZ

Istanbul Teknik Üniversitesi, Avrasya Yer Bilimleri Enstitüsü, TR–34469 Ayazaga, Istanbul, Turkey

VEYSEL ISIK

Department of Geological Engineering, Ankara University, TR–06100 Ankara, Turkey

ABSTRACT

A hydrothermal breccia zone 6 km long and 2 km wide, crossed by quartz–tourmaline veins, occurs to the south of the Late Cretaceous Kerkenez granite–monzonite massif in the northern part of the Central Anatolian Crystalline Complex, Yozgat, Turkey. This breccia zone is characterized by numerous veins, a few millimeters to 1 meter in width, and display typical microtectonic features of multiple brecciation. Trace amounts of albite, K-feldspar, epidote, muscovite and rutile are associated with quartz and tourmaline. Petrographic features indicate three successive stages of tourmaline generation. The first generation is represented by feruvite, and the second and third generations consist of schorl. These distinct generations of tourmaline show successive enrichment in Al and Na, and depletion in Ti and Ca. The Na/(Na + Ca) values vary in the range 0.41–0.49 in the first generation, and 0.53–0.86 and 0.91–0.99 in the second and third generations. The development of the breccia zone and formation of three successive generations of tourmaline are most probably related to fluid-assisted brecciation and infiltration of low- to medium-pH hydrothermal fluids under subsolidus conditions. Successive enrichment in Na and Al in the younger generations is ascribed to late-stage fractionation in the B-rich granitic source.

Keywords: tourmaline, composition, hydrothermal breccia, Kerkenez, central Anatolia, Turkey.

SOMMAIRE

Nous décrivons une zone de brèche hydrothermale exposée sur une distance de 6 km et une largeur de 2 km et traversée par des veines à quartz–tourmaline au sud du massif granitique–monzonitique de Kerkenez, d'âge crétacé supérieur, situé dans la partie nord du complexe cristallin de l'Anatolie centrale, près de Yozgat, en Turquie. Dans cette zone bréchifiée, les nombreuses veines varient de quelques millimètres à un mètre en largeur, et démontrent les textures microtectoniques typiques de bréchification multiple. Des traces d'albite, de feldspath potassique, d'épidote, de muscovite et de rutile sont présentes. Les attributs pétrographiques indiquent trois stades de formation de la tourmaline. La première génération a donné la feruvite, tandis que la deuxième et la troisième génération ont produit le schorl. Dans l'ensemble, ces trois générations de tourmaline définissent un enrichissement successif en Al et Na, et un appauvrissement en Ti et Ca. Les valeurs de Na/(Na + Ca) varient entre 0.41 et 0.49 dans la première génération, et dans les intervalles 0.53–0.86 et 0.91–0.99 dans les générations suivantes. Le développement de la zone bréchifiée et la formation de trois générations successives de tourmaline résulteraient d'une libération de la phase fluide et de l'infiltration de fluides de pH faible à modéré en dessous du solidus. L'enrichissement progressif en Na et Al dans les générations tardives serait dû au fractionnement tardif d'un magma granitique borifère.

(Traduit par la Rédaction)

Mots-clés: tourmaline, composition, brèche hydrothermale, Kerkenez, Anatolie centrale, Turquie.

§ mcgoncu@metu.edu.tr

Introduction

Tourmaline is the most common expression of boron in natural rocks, occurring mostly as an accessory phase. Boron is a highly incompatible and fluid-mobile element that is of low abundance in crustal and mantle rocks (*e.g.,* Ryan & Langmuir 1993, Chaussidon & Marty 1995, McDonough & Sun 1995, Taylor & McLennan 1985). The formation of tourmaline (~3 wt% B_2O_3) requires the effective concentration of boron, mostly by magmatic differentiation and fluid-dominated processes. Consequently, tourmaline can locally become the main constituent of particular rock-types, such as tourmalinite (*e.g.*, Slack *et al.* 1984), tourmaline-bearing granite, pegmatite, greisen (*e.g.,*Trumbull & Chaussidon 1999), quartz–tourmaline breccias and breccia pipes within granites (*e.g.*, London & Manning 1995, Williamson *et al.* 2000) and metasomatic blackwalls around eclogite knockers within serpentinite mélanges (*e.g.,* Altherr *et al.* 2004, Marschall *et al.* 2006). Several features, such as a complex composition, the common presence of compositional zoning, and resistance to chemical diffusion and alteration make tourmaline an important chemical monitor of changing conditions during its growth (Henry & Guidotti 1985, Henry & Dutrow 1992, 1996). Although there are several studies on tourmalines and tourmalinites, studies on tourmaline breccias are relatively rare. Tourmaline breccias are generally attributed to magmatic–hydrothermal systems related to magma emplacement. Generally, mechanisms of formation include: collapse of the overlying rocks due to dissolution action of hydrothermal fluids (Sillitoe & Sawkins 1971), explosive ascent of hydrothermal solutions to the surface and fracturing the overlying rocks (Warnaars *et al.* 1985), explosive loss of volatiles (London & Manning 1995), rapid uplift, unroofing by erosion and exsolution of magmatic fluids (Skewes *et al.* 2003).

In this paper, we describe a zone of quartz–tourmaline breccias within the Kerkenez granite–monzonite massif, Sorgun, central Anatolia, Turkey, and document compositional variations in the tourmaline-group minerals. These data are discussed in terms of the formation of the quartz–tourmaline breccias. We suggest that the tourmaline–quartz breccias were formed in an open system following crystallization of the magma.

Regional Geological Setting

Turkey constitutes an important part of Alpine–Himalayan collision system and comprises several oceanic and continental terranes with different geological features (Göncüoğlu *et al.* 1997). Neotethys opened in this region during the Triassic and closed in the Late Cretaceous (Sengör & Yilmaz 1981, Göncüoğlu *et al.* 1997). During the closure of the northern branch of Neotethys, represented by the Izmir – Ankara – Erzincan Suture Belt, allochthonous nappes of ophiolitic sequences and tectonic mélanges were thrust southward onto the passive margin of the Tauride–Anatolide Platform (Göncüoğlu *et al.* 2000). This led to intense metamorphism and magmatism in central Anatolia. The assemblages of magmatic, metamorphic and ophiolitic rocks in central Anatolia are defined as the Central Anatolian Crystalline Complex by Göncüoğlu *et al.* (1991). The rocks that crop out within the Central Anatolian Crystalline Complex include metamorphic rocks, mélange slices and felsic to intermediate plutonic rocks known as the Central Anatolian Granitoids (Göncüoğlu *et al.* 1991). The plutonic rocks comprise granitic to syenitic rocks that are products of either syn-collisional or post-collisional magmatism (Göncüoğlu *et al.* 1991, 1992, 1993). They are in general represented by I-, S-, A-type granite rocks ranging in age from 70 to 80 Ma (*e.g.,* Erler *et al.* 1991, Akiman *et al.* 1993, Göncüoğlu & Türeli 1993, Kadioglu & Gülec 1999, Ilbeyli *et al.* 2004, Köksal *et al.* 2004, Boztuğ *et al.* 2007a, b).

The metamorphic rocks range in grade from the upper greenschist to upper amphibolite–granulite facies (Seymen 1981, Whitney & Dilek 2001). The timing of metamorphism is constrained by regional geological relationships and U–Pb monazite dating at 85 Ma (Göncüoğlu 1982, Whitney & Hamilton 2004). The metamorphic rocks are tectonically overlain by Late Cretaceous mélanges with dismembered and partially preserved ophiolitic rocks (Yaliniz & Göncüoğlu 1999). These basement rocks are disconformably overlain by uppermost Maastrichtian clastic sediments. The Eocene carbonates, volcanic rocks and clastic rocks rest with an angular unconformity on the older rocks. The Neogene sediments are represented by Oligocene–Miocene evaporites and clastic rocks and Miocene–Pliocene continental clastic rocks (Göncüoğlu *et al.* 1991).

The Kerkenez Granite–Monzonite Massif and Quartz–Tourmaline Breccias

The Yozgat Batholith constitutes the largest intrusive complex of the overall post-collisional Central Anatolian magmatism. It has distinct units produced by mixing-mingling between underplating mafic and crustal felsic magmas. Geochemical data show that the Yozgat Batholith formed by partial melting in a post-collisional, crust-thickening environment (Boztuğ 2000). The Kerkenez granite–monzonite massif is located at the southeastern border of the Yozgat Batholith and is exposed over an area of 160 km^2 (Fig. 1). The dominant rocks of Kerkenez granite–monzonite massif are quartz monzonite, monzogranite and monzonite. The Kerkenez massif intrudes the Late Cretaceous ophiolitic mélange (radiolarite, pelagic limestone and basalt) and small stocks of the intrusion cross-cut the metamorphic rocks. The biotite K–Ar ages obtained from the quartz monzonites and monzogranites of the southwestern part of the Kerkenez complex are between

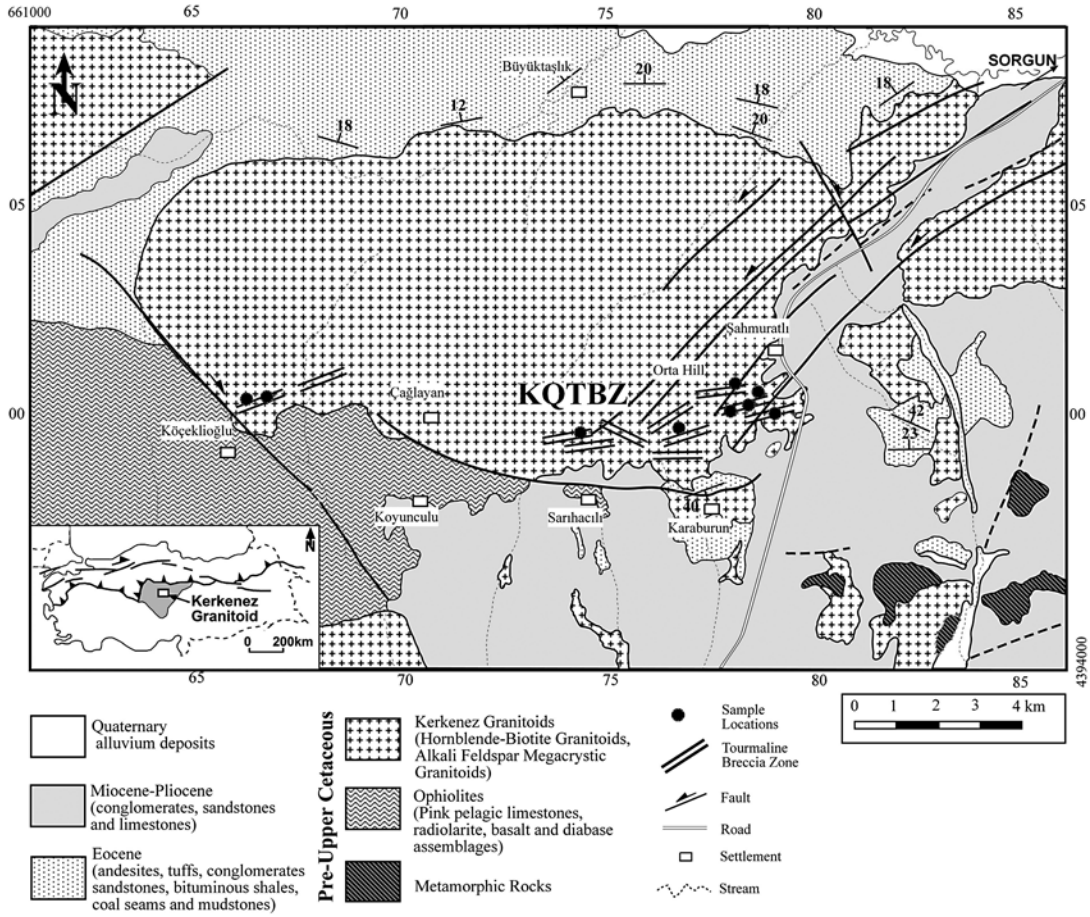

FIG. 1. Geological map of the Kerkenez granitic pluton with location of samples (modified after Göncüoğlu *et al*. 1994). The inset shows the location of Central Anatolian Crystalline Complex in Turkey, and the location of the Kerkenez granite–monzonite massif within it.

68 and 71 Ma (Boztuğ *et al*. 2007b). These ages are in accordance with the hornblende Ar–Ar ages of about 72 Ma, recently obtained from the granitic rocks in the study area that host the Kerkenez Quartz–Tourmaline Breccia Zone (Isik *et al*. 2008).

The main structural features of the Kerkenez granite–monzonite massif are the NE–SW striking dip-slip faults. A breccia zone ~6 km long and up to 2 km wide (the Kerkenez Quartz–Tourmaline Breccia Zone, KQTBZ) occurs within the southern part of the Kerkenez granite–monzonite Massif. The vertically dipping (~80–85°) KQTBZ continues several kilometers with a NE–SW trend and can be traced along the western and southwestern margins of the massif in the form of thin tourmaline-filled veins and networks. Faults along the zone are generally coated with tourmaline, and the boundaries between the host granite are sharp. Tourmaline-filled veins are abundant along the zone, and cataclastic deformation is clearly visible. Outcrop relations are relatively poor owing to soil cover. Nonetheless, the zone rocks are generally found in the field as fragmented blocks that range up to 1 meter across. The blocks of the host granite range from 30 to 250 cm across. Depending on the relative proportions of the quartz–tourmaline cements to fragments of the host granite, three different rock units can be distinguished along the zone: quartz–tourmaline rocks, tourmaline breccias and quartz–tourmaline veins. It should be noted that this subdivision is only for descriptive purposes; these rocks are closely related to each other. *Quartz–tourmaline rocks* display a massive texture and have a characteristic black color; they contain few or no granitic fragments. Tourmaline, the dominant mineral, makes up 70–90% of the rock by volume. *Tourmaline*

breccias show a brecciated texture, suggestive of brittle deformation and formation under subsolidus conditions. Breccias consist of angular–subangular granitic fragments. Dislocated blocks of the host rock and irregular brecciated texture with network of tourmaline–quartz veinlets are common. The volume of tourmaline is limited compared to the quartz–tourmaline rocks. *Quartz–tourmaline veins* are very abundant and occur in granites around the main quartz–tourmaline breccia zone in form of thin veins or networks with variable widths ranging from several mm to 30 cm. A general view of the rocks can be seen in Figure 2.

Analytical Techniques

Tourmaline compositions were determined in Heidelberg University (Germany) with a CAMECA SX–51 electron microprobe equipped with five wavelength-dispersive spectrometers and an additional Si–Li detector (Oxford Instruments). Operating conditions were 15 kV accelerating voltage and 20 μA beam current. For the analysis of tourmaline, the beam size was defocused to 5 μm. Synthetic and natural oxide and silicate standards were used for calibration: MgO for Mg (20 s), albite for Na (10 s), Al_2O_3 for Al (10 s), wollastonite for Si (10 s) and Ca (10 s), orthoclase for K (10 s), TiO_2 for Ti (20 s), Cr_2O_3 for Cr (20 s), rhodonite for Mn (10 s), and Fe_2O_3 for Fe (10 s). Analytical uncertainties are ±1% relative for major elements and ±5% relative for minor elements. A PAP correction was applied to the raw data (Pouchou & Pichoir 1985).

The structural formula of tourmaline is $XY_3Z_6(T_6O_{18})(BO_3)_3V_3W$ (*e.g.,* Hawthorne & Henry 1999), where X = (Ca, Na, K, vacancy), Y = (Li, Mg, Fe^{2+}, Mn^{2+}, Al, Cr^{3+}, V^{3+}, Fe^{3+}, Ti^{4+}), Z = (Mg, Al, Fe^{3+}, V^{3+}, Cr^{3+}), T = (Si, Al, B), V = (OH, O) and W = (OH, F, O). Abundances of Li, B, F and H and the ratio $Fe^{3+}/\Sigma Fe$ cannot be measured with the electron microprobe. These unknowns lead to problems in calculating a formula. For the Kerkenez tourmalines, a Si = 6 normalization procedure was applied, total Fe is considered as divalent, and three B atoms per formula unit were assumed (*e.g.,* Henry & Dutrow 1996, Clark 2007). With this procedure, one assumes that the tetrahedral site is totally

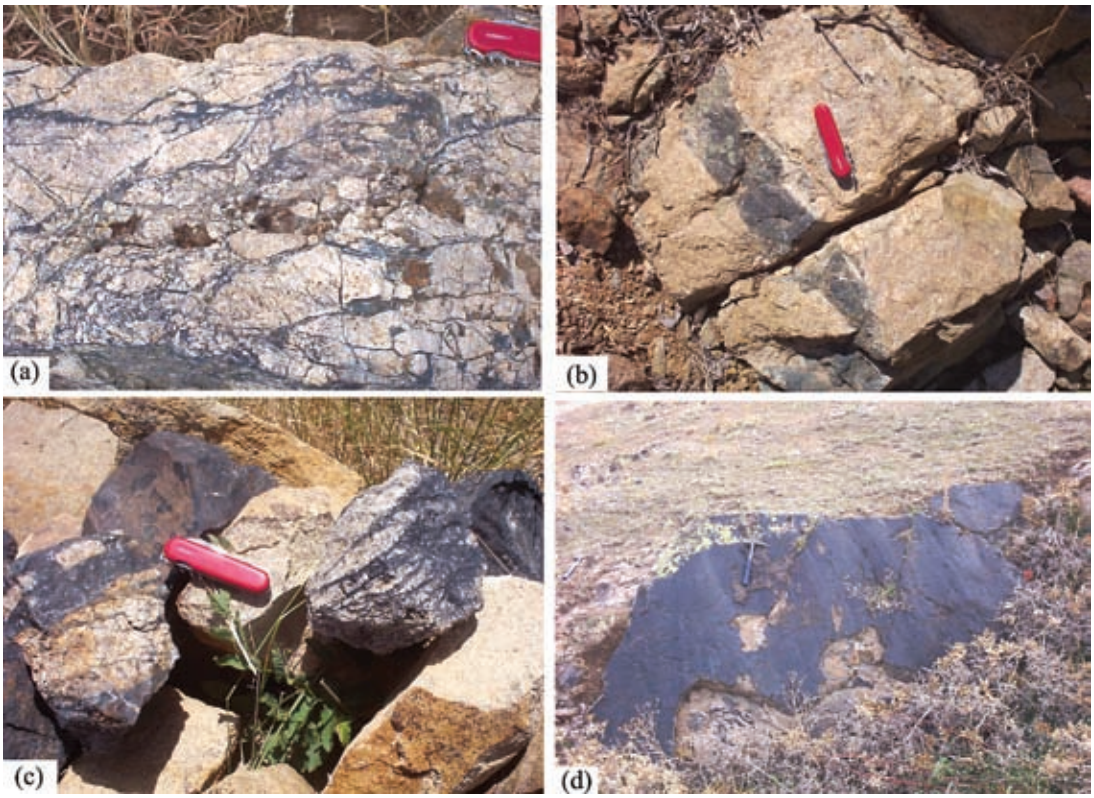

Fig. 2. Field images of tourmaline breccias in the Kerkenez granite–monzonite massif. (a) Highly fractured granitic rock with abundant cross-cutting veins of tourmaline. (b) A tourmaline vein ~15 cm thick within the granite. (c) Tourmaline breccia and host-rock fragments. (d) A tourmaline-coated fault surface indicating reactivation of faults after tourmaline formation.

occupied by Si. In cases of the presence of tetrahedrally coordinated boron and Al, this will be an overestimate. On the other hand, the other schemes of normalization (24.5 atoms of oxygen, $T + Z + Y = 15$, *etc.*) result in Si contents above 6 cations per formula unit.

Representative compositions are reported in Table 1; the full set of data is available from the Depository of Unpublished Data [document Kerkenez CM47_787].

Petrography and Tourmaline Composition

Petrographically, the host granitic rocks can be defined as granites, quartz monzonites and monzonites. They are phaneritic, holocrystalline and weakly porphyritic to equigranular. The main constituents are plagioclase, orthoclase, hornblende and quartz. Biotite is rare compared to other constituents. Accessory minerals are apatite, titanite, zircon, allanite and fluorite. No tourmaline is present within the undeformed host-rocks. The KQTBZ rocks are generally fine-grained (~100 μm). Quartz and clasts of host rocks display fractures and angular shapes; sizes range from 1.5 to 0.05 mm. Tourmaline forms grains of variable sizes (5 to 0.01 mm). The tourmaline breccias are mainly composed of quartz- and orthoclase-dominant angular fragments of granitic rock and minerals and a microcrystalline matrix. The matrix is composed of light green acicular grains of tourmaline and includes angular to subrounded porphyroclasts of tourmaline of former generations. The tourmaline in veins is microcrystalline and locally cryptocrystalline. Multiple deformation events can be differentiated in the tourmaline rocks. The first phase of cataclastic deformation and tourmaline formation was followed by other fracturing phases, which are reflected in deformation of both quartz and tourmaline. A thin-section view of the KQTBZ rocks is presented in Figure 3.

Texturally, three different generations (groups) of tourmaline are distinguished within the KQTBZ rocks. Cross-cutting relationships suggest that Group A represents the oldest and Group C represents the youngest generation. In accordance with the petrographic observations, representation of the microprobe data on the Ca–X_{vac}–Na+(K) triangular diagram (Fig. 4) of Hawthorne & Henry (1999) supports the petrographic observations and shows that there are three chemically distinct groups of tourmaline. Group-A tourmaline consists of calcic feruvite, whereas schorl is found in Groups B and C (Fig. 5).

The first generation (Group A) compositionally corresponds to feruvite. It is composed of accumulations of subhedral grains of tourmaline 0.05–2 mm in

TABLE 1. REPRESENTATIVE COMPOSITIONS OF TOURMALINE IN THE QUARTZ–TOURMALINE BRECCIAS

Anal.	12	17	45a	46a	47a	51a	66a	2	13	3a	4a	10a	14a	21a	6	9	31	1a	12a	16a	43a
Type	Fer	Fer	Fer	Fer	Fer	Fer	Fer	Srl	Srl	Srl	Srl	Srl	Srl	Srl	O-Srl	Srl	Srl	Srl	Srl	Srl	O-Srl
Group	A	A	A	A	A	A	A	B	B	B	B	B	B	B	C	C	C	C	C	C	C
SiO_2	35.08	35.08	35.19	34.62	34.94	35.08	34.77	34.99	35.64	34.87	34.28	34.95	34.93	35.50	36.30	35.73	35.61	35.97	35.80	35.71	36.30
TiO_2	0.80	0.63	0.57	0.74	0.70	0.55	0.68	0.41	0.28	1.27	0.90	0.82	0.22	0.20	0.01	0.06	0.08	0.07	0.50	0.23	0.02
Al_2O_3	21.93	21.91	23.66	22.25	22.24	23.31	22.44	25.69	26.41	25.96	24.45	27.16	27.64	28.91	30.25	28.96	28.91	29.89	29.54	30.18	29.01
Cr_2O_3	0.01	0.00	0.05	0.01	0.04	0.00	0.00	0.02	0.01	0.00	0.00	0.00	0.03	0.00	0.00	0.00	0.00	0.00	0.01	0.00	0.00
FeO	17.74	17.35	15.67	16.73	17.38	18.04	17.83	17.60	14.99	16.34	20.31	15.22	16.67	14.51	15.42	15.77	16.45	12.80	15.03	14.27	13.95
MnO	0.05	0.05	0.05	0.09	0.07	0.13	0.07	0.07	0.06	0.07	0.03	0.07	0.03	0.08	0.02	0.02	0.07	0.01	0.08	0.05	0.16
MgO	6.07	6.76	6.73	6.53	6.37	5.38	6.34	3.88	5.53	3.95	2.79	4.08	3.19	3.66	2.66	3.30	2.82	4.23	3.64	3.36	3.80
CaO	2.73	3.05	2.64	2.85	2.72	2.92	2.85	1.40	1.59	1.02	1.71	0.87	0.87	0.68	0.30	0.43	0.37	0.44	0.23	0.15	0.20
Na_2O	1.34	1.18	1.38	1.24	1.31	1.20	1.29	2.00	1.94	2.15	1.84	2.26	2.25	2.28	2.36	2.46	2.47	2.34	2.35	2.26	2.25
K_2O	0.04	0.04	0.02	0.02	0.04	0.05	0.04	0.07	0.05	0.06	0.03	0.04	0.04	0.04	0.03	0.03	0.04	0.03	0.00	0.00	0.02
Total	85.79	86.05	85.96	85.08	85.81	86.66	86.31	86.13	86.50	85.69	86.34	85.47	85.87	85.86	87.35	86.76	86.82	85.78	87.18	86.21	85.71
Si *apfu*	6.00	6.00	6.00	6.00	6.00	6.00	6.00	6.00	6.00	6.00	6.00	6.00	6.00	6.00	6.00	6.00	6.00	6.00	6.00	6.00	6.00
Ti	0.10	0.08	0.07	0.10	0.09	0.07	0.09	0.05	0.04	0.16	0.12	0.11	0.03	0.03	0.00	0.01	0.01	0.01	0.06	0.03	0.00
Al	4.42	4.42	4.75	4.55	4.50	4.70	4.56	5.19	5.24	5.27	5.04	5.50	5.60	5.76	5.89	5.73	5.74	5.88	5.84	5.98	5.65
Cr	0.00	0.00	0.01	0.00	0.01	0.00	0.00	0.00	0.00	0.00	0.00	0.00	0.00	0.00	0.00	0.00	0.00	0.00	0.00	0.00	0.00
Fe^{2+}	2.54	2.48	2.23	2.43	2.50	2.58	2.57	2.52	2.11	2.35	2.97	2.19	2.40	2.05	2.13	2.22	2.32	1.79	2.11	2.01	1.93
Mn	0.01	0.01	0.01	0.01	0.01	0.02	0.01	0.01	0.01	0.01	0.00	0.01	0.00	0.01	0.00	0.00	0.01	0.00	0.01	0.01	0.02
Mg	1.55	1.72	1.71	1.69	1.63	1.37	1.63	0.99	1.39	1.01	0.73	1.04	0.82	0.92	0.66	0.83	0.71	1.05	0.91	0.84	0.94
Ca	0.50	0.56	0.48	0.53	0.50	0.54	0.53	0.26	0.29	0.19	0.32	0.16	0.16	0.12	0.05	0.08	0.07	0.08	0.04	0.03	0.04
Na	0.44	0.39	0.46	0.42	0.44	0.40	0.43	0.67	0.63	0.72	0.62	0.75	0.75	0.75	0.76	0.80	0.81	0.76	0.76	0.74	0.72
K	0.01	0.01	0.00	0.00	0.01	0.01	0.01	0.02	0.01	0.01	0.01	0.01	0.01	0.01	0.01	0.01	0.01	0.01	0.00	0.00	0.00
B	3.00	3.00	3.00	3.00	3.00	3.00	3.00	3.00	3.00	3.00	3.00	3.00	3.00	3.00	3.00	3.00	3.00	3.00	3.00	3.00	3.00
Fe#	0.62	0.59	0.57	0.59	0.60	0.65	0.61	0.72	0.60	0.70	0.80	0.68	0.75	0.69	0.76	0.73	0.77	0.63	0.70	0.70	0.67
Na#	0.47	0.41	0.49	0.44	0.47	0.43	0.45	0.72	0.69	0.79	0.66	0.82	0.82	0.86	0.93	0.91	0.92	0.91	0.95	0.96	0.95

Fe#: Fe/(Fe + Mg); Na#: Na/(Na + Ca). Symbols: Fer: feruvite, Srl: schorl, O-Srl: "Oxy-schorl".

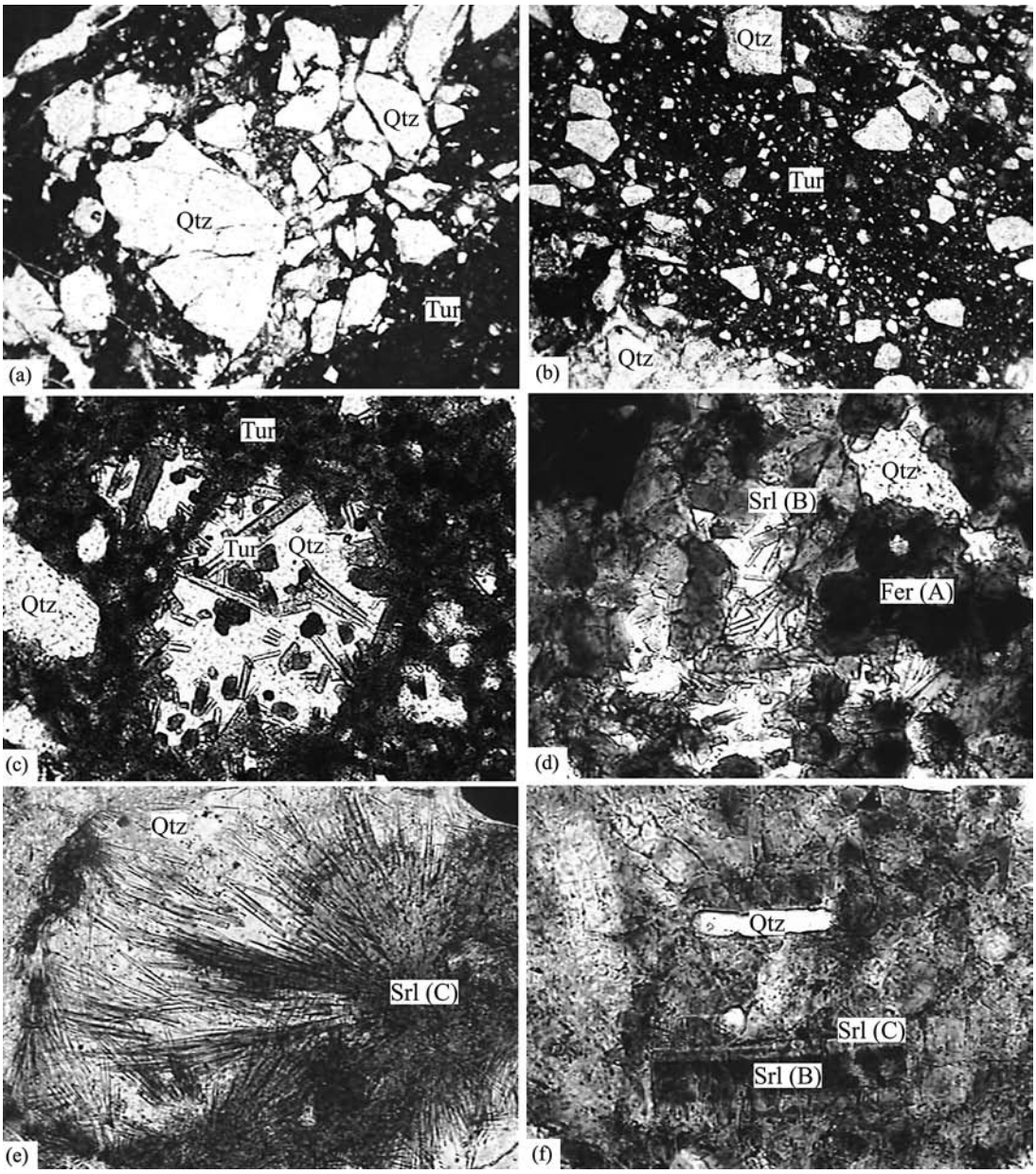

FIG. 3. (a, b) Photomicrographs showing the intense brittle deformation in quartz–tourmaline breccias. Black matrix is made up of microcrystalline tourmaline. (c) Coarse-grained tourmaline matrix and prismatic tourmaline overgrowths. (d) Group A (feruvite) and Group B (schorl). (e) Acicular and radiating Group C schorl overgrowths. (f) Compositionally zoned prismatic tourmaline showing the core–rim relationship between different generations of tourmaline. (Fer: Feruvite, Qtz: Quartz, Srl: Schorl, Tur: Tourmaline); A, B, C: group names.

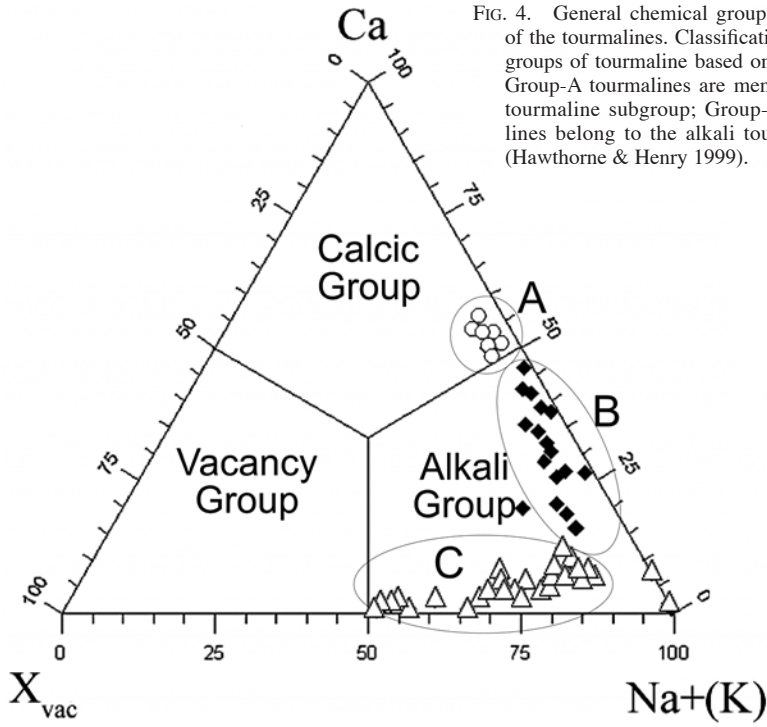

FIG. 4. General chemical groups and subdivisions of the tourmalines. Classification of the principal groups of tourmaline based on *X*-site occupancy. Group-A tourmalines are members of the calcic tourmaline subgroup; Group-B and -C tourmalines belong to the alkali tourmaline subgroup (Hawthorne & Henry 1999).

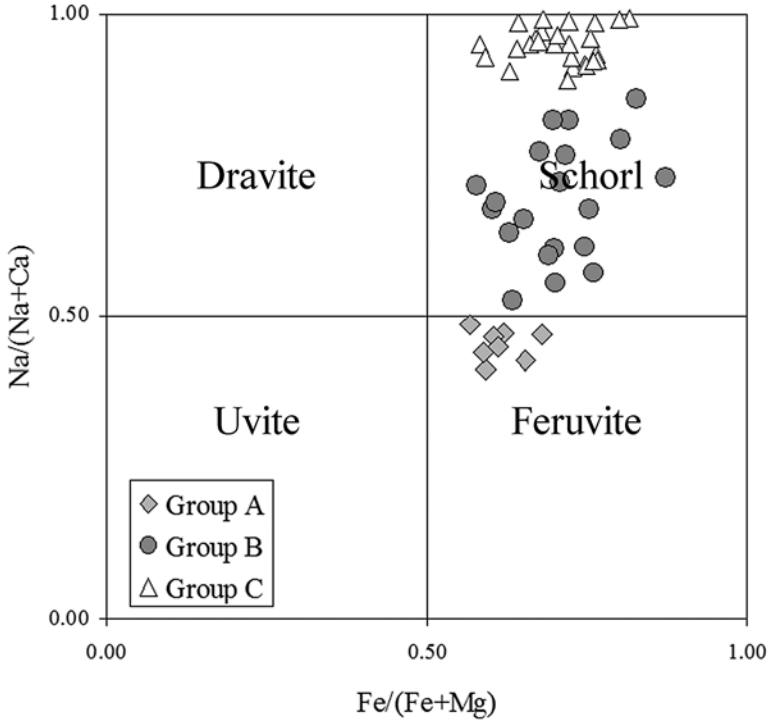

FIG. 5. Plot of Na/(Na + Ca) *versus* Fe/(Fe + Mg) in tourmalines of Group A (feruvite) and Groups B and C (schorl).

size. They form clusters of short prismatic crystals and exhibit a granular texture. They are dark brown to dark blue in color and less plentiful compared to other tourmaline generations. The second generation (Group B) encloses and replaces Group A and forms an overgrowth on host-rock minerals. Group-B tourmaline is green to bluish green in color, and schorl in composition. The third generation of tourmaline (Group C, also schorl in composition) is fine grained (0.5–0.05 mm), pale green and acicular. It occurs commonly in the matrix and fractures and cross-cuts earlier-formed tourmaline. This relation is clearly observed in the back-scattered electron image (Fig. 6), where the Group-C schorl cross-cuts dark-colored Group-A feruvite.

Distinct groups of tourmaline display marked compositional differences. Systematically, Na and Al contents increase from Group A to C, whereas Ti and Ca contents decrease (Table 1). The Na/(Na + Ca) value increases from 0.41–0.49 in Group A through 0.53–0.86 in Group B to 0.91–0.99 in Group C (Table 1). The TiO_2 contents systematically decreases from 0.55 to 0.80 wt% in Group A to 0.03–0.55 wt% in Group C. The ratio Fe/(Fe + Mg) increases from Group A to Groups B and C, in which the value is the same.

Compositional variations from different groups are best described by the exchange vector $NaAlCa_{-1}Mg_{-1}$ (Fig. 7); changes from Group B to Group A are more consistent with operation of the exchange vectors $CaMg_3OH\square_{-1}Al_{-3}O_{-1}$ and $CaMg_2\square_{-1}Al_{-2}$ (Fig. 8). Differentiation within the groups can also be described by these exchange reactions. Apart from Group A and B, Group C shows a reverse order, which is more consistent with the exchange vector $\square AlNa_{-1}Mg_{-1}$. According to the exchange vector, the proportion of vacancies and Al increases, and that of Na and Mg decreases within Group C (Fig. 6).

Discussion and Conclusions

The KQTBZ rocks are characterized by cataclastic-brecciated textures and a dark color due to the crystallization of tourmaline. The presence of an irregular brecciated texture with non-oriented quartz fragments, the angular and weakly rounded character of the rock–mineral fragments, a paucity of corrosion and of tourmaline crystallization in the Kerkenez monzonite–granite indicate that the breccias formed by fluid-assisted (hydraulic) brecciation (Lorilleux *et al*. 2002).

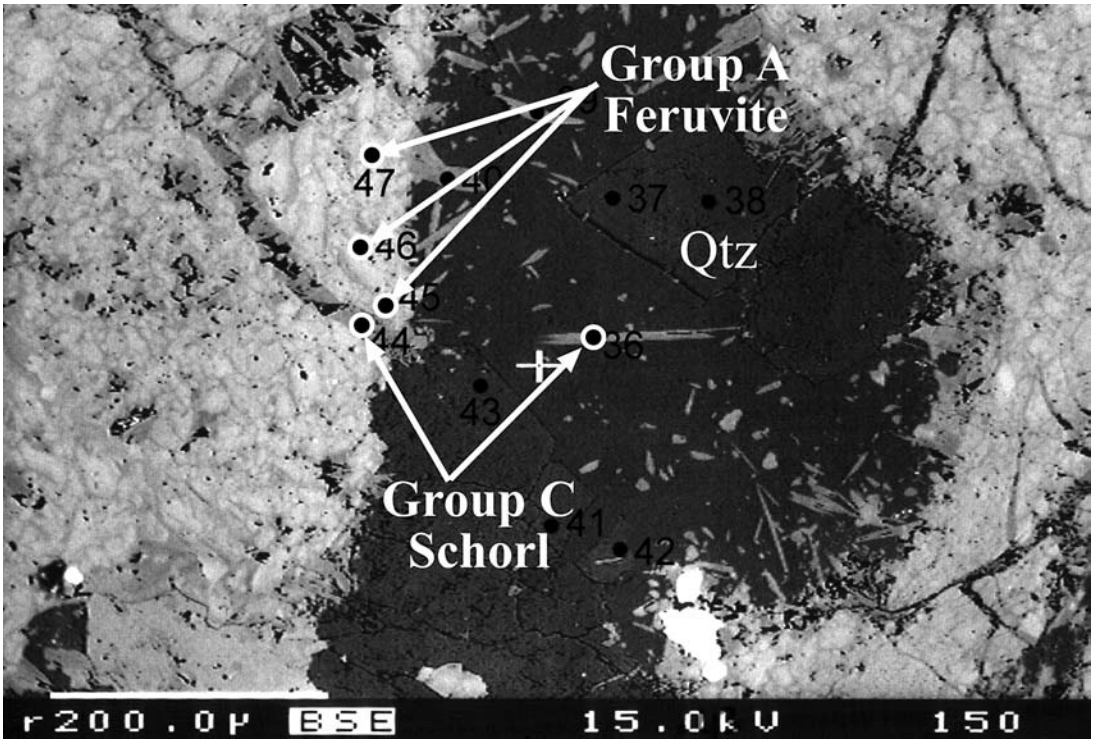

FIG. 6. Back-scattered electron image showing EMPA points and cross-cutting relationship of tourmaline groups. Younger Group-C schorl cross-cuts dark-colored Group-A feruvite and display acicular intergrowths. Dots indicate analyzed points; the dark colored mineral is quartz.

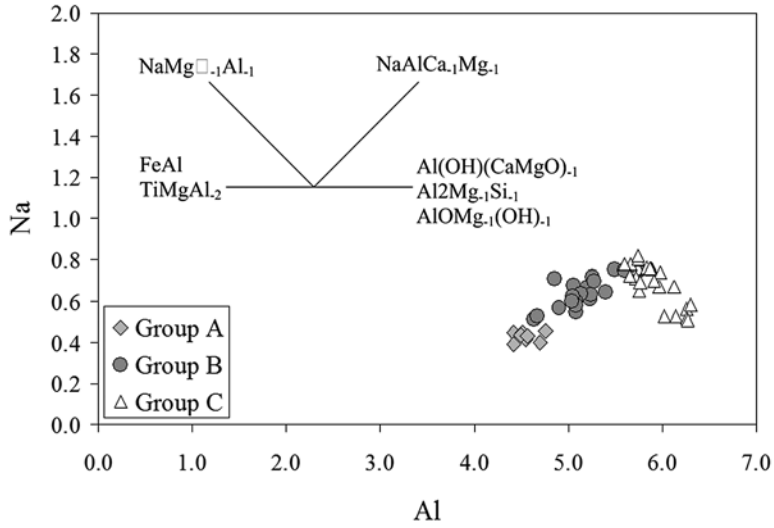

FIG. 7. Plot of Na *versus* Al. The vectors represent the possible exchange-operator that could have been effective in these tourmalines.

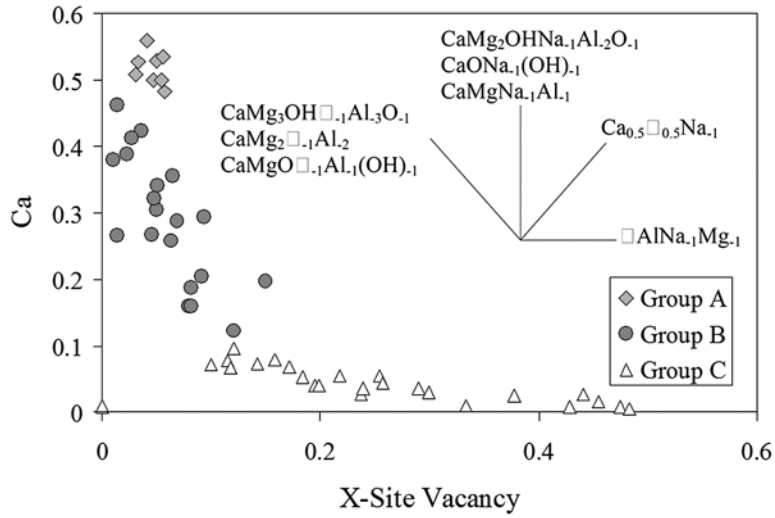

FIG. 8. Plot of Ca *versus* $^{X}\square$. The vectors represent the possible exchange-operators that could have been effective in these tourmalines.

There were multiple episodes of tectonic movement and associated brecciation in the Kerkenez monzonite–granite. Tourmaline-rich breccias within the KQTBZ seems to be cataclastically deformed rocks that lie close to faults and formed by penetration of boron-rich fluids into fault zones, hydraulic brecciation and crystallization of tourmaline within the matrix. The general characteristics of the quartz–tourmaline rocks indicate that they formed in an environment represented by a high fluid:rock ratio. A high activity of fluid and paucity of host-rock fragments indicate that these rocks formed in larger open spaces within the Kerkenez monzonite–granite. The hydrothermal solutions may represent the hydrothermal fluids related to the crystallization of the Kerkenez monzonite–granite or they could have been derived externally. However, no tourmaline is found

in the host Kerkenez monzonite–granite. The stability of tourmaline in aqueous solutions primarily depends on pH and B content of the fluid and on temperature. Weisbrod *et al*. (1986) and London *et al*. (1989) have demonstrated that the minimum content of boron necessary for tourmaline crystallization increases with pH and temperature, and tourmaline synthesis was not possible at high B contents under relatively high pH. As tourmaline is a peraluminous species, we argue that the Kerkenez quartz–tourmaline breccias are formed from the low- to medium-pH hydrothermal fluids.

Formation of the KQTBZ requires infiltration of enormous volumes of boron-rich fluids. High concentrations of boron in granites facilitate emplacement at shallow levels. Because of the high volatile content, the magma can impose high fluid pressures on the host rocks by its degassing (London *et al*. 1989).

The presence of a magmatic source, cataclastic deformation, intense faulting and fracturing within the KQTBZ indicate that tourmaline crystallization took place at shallow depths within the continental crust. Such an intrusion seems to be a cupola, *i.e*., a finger-like intrusion emplaced at a depth of few kilometers (Titley & Beane 1981, Shinohara *et al*. 1995, Guillou-Frottier & Burov 2003). Concentration of fractures and faults around plutonic apices allows circulation of hydrothermal and magmatic fluids. The small diameter of the cupola provides lateral cooling from the host rocks and can enable brittle deformation around and above the apex (Guillou-Frottier & Burov 2003). Breccia pipes generally occur in such systems. However, the KQTBZ occurs as an elongate zone parallel to the regional structural trend (NE–SW) (Dirik & Göncüoğlu 1996, Dirik *et al*. 1999). The process considered to have promoted fluid infiltration before formation of a breccia pipe is the tectonic activity that produced shear zones within the Kerkenez monzonite–granite.

Shear zones can act as conduits for focused flow of overpressured fluids as the fluid phase moves from high- to low-pressure areas and slows down in the strongly fractured low-pressure regimes (Helgeson 1992, Ridley 1993). Such a scenario could have led to fracturing and fracture propagation within the solidified host pluton. Flow along a negative temperature-gradient from the intrusion into the host rock tends to crystallize tourmaline from boron-bearing fluids (Norton & Dutrow 2001).

Operation of the same exchange-vectors and the chemical similarity of Group A and B tourmalines indicate that faults became reactivated after a short time, and then Group-B tourmalines formed, or these two groups of tourmalines formed contemporaneously during the first fracturing and fluid-injection event. Feruvite formation is reported to be controlled by the reaction of hydrothermal fluids with Ca-rich minerals in the host rocks (Grice & Robinson 1989, Jiang *et al*. 1996). The latest generation of tourmaline, Group C, is distinctly more evolved than Group A and B. The gradual change in the chemical compositions of the different generations of tourmaline implies that the source of fluid giving way to their crystallization were undergoing fractionation and becoming successively enriched in Na and Al. General chemical characteristics of tourmaline groups indicate that the internal fractionation and differentiation of the magmatic source continued during the formation of the KQTBZ. This situation might be explained by the closure of the system, during which hydrothermal fluids injected into faults and fractures, and sealed the faults by new crystallization and produced new accumulations of fluid pressure, which led to reactivation of the faults (Clark & James 2003). In the KQTBZ, this process appears to be has been repeated several times. These stages of opening, sealing and reopening of veins produced three different generations of tourmaline. The most likely mechanism of generation for the Kerkenez monzonite–granite is shown in Figure 9. We plan more detailed analytical work and boron isotope analysis, to establish the source and the nature of the magma and the boron.

Acknowledgements

This study had been financially support by TUBITAK (YDBAG–102Y123). We gratefully acknowledge the fruitful discussions with Steve Mittwede and Fatma Toksoy Köksal, and the constructive comments of Mark Welch on the earlier draft of this manuscript. Thanks are also due to Rainer Altherr for the access to the electron-microprobe facility in Heidelberg University. We also acknowledge gratefully the comments of Associate Editor Milan Novák, Robert F. Martin and referees Pavel Uher and Didier Béziat.

References

Akiman, O., Erler, A., Göncüoğlu, M.C., Gülec, N., Geven, A., Türeli, T.K. & Kadioglu, Y.K. (1993): Geochemical characteristics of the granitoids along the western margin of the Central Anatolian Crystalline Complex and their tectonic implications. *Geol. J.* **28**, 371-382.

Altherr, R., Topuz, G., Marschall, H., Zack, T. & Ludwig, T. (2004): Evolution of a tourmaline-bearing lawsonite eclogite from Elekdag area (Central Pontides, N Turkey): evidence for infiltration of slab-derived B-rich fluids during exhumation. *Contrib. Mineral. Petrol.* **148**, 409-425.

Boztuğ, D. (2000): S-I-A intrusive associations: geodynamic significance of synchronism between metamorphism and magmatism in Central Anatolia, Turkey. *In* Tectonics and Magmatism in Turkey and the Surrounding Area (E. Bozkurt, J.A. Winchester & J.D.A. Piper, eds.). *Geol. Soc., Spec. Publ.* **173**, 441-458.

Boztuğ, D., Harlavan, Y., Arehart, G.B., Satir, M. & Avci, N. (2007b): K–Ar age, whole-rock and isotope geochem-

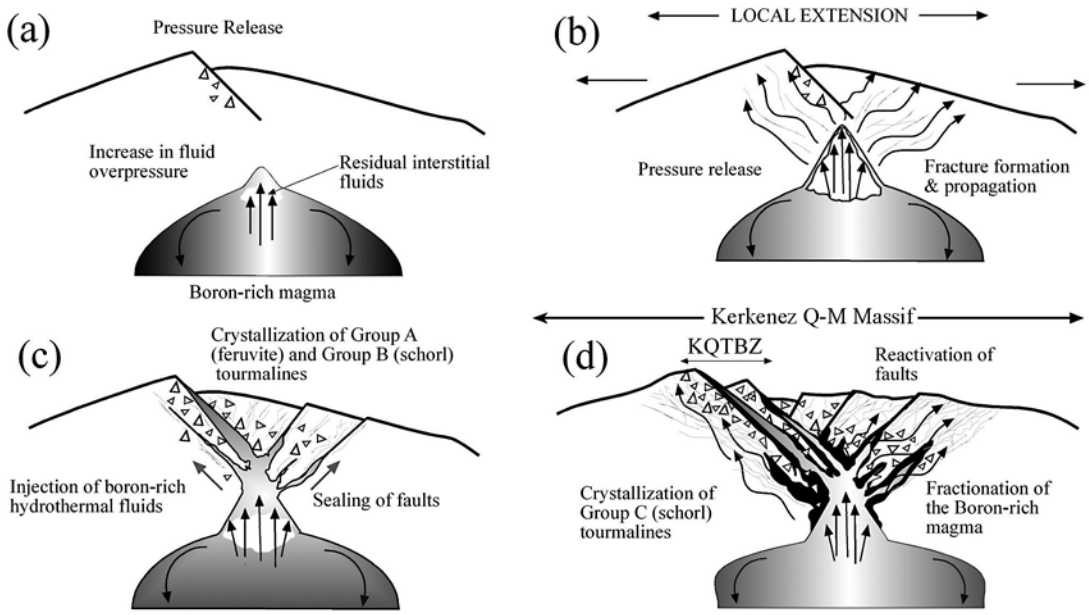

FIG. 9. (a) Formation of cupola and pressure release by regional tectonic activity. Upwelling and crystallization led to separation of the interstitial fluid and increase in fluid overpressure. (b) Local extensional regime due to the emplacement of the boron-rich magma. Faulting and fracturing created a low-pressure regime in the host rock. Infiltration of boron-rich fluids into the low-pressure regime (host rock) triggered fracture propagation and enlarged the main deformation by further brecciation and fracture formation and propagation. (c) Crystallization of Group-A feruvite as the first phase and Group-B as a secondary phase. The chemical similarity of Group A and B tourmalines indicate that faults were reactivated after a short time, and Group-B tourmalines formed, or they formed together during the first faulting. Crystallization of tourmaline and quartz led to sealing of open spaces. (d) Further episodes of brecciation and crystallization of Group-C schorl. Sealing isolated the magma and allowed more fractionation and further build-up of the fluid pressure. Regional tectonic activities and increasing fluid overpressures led to reactivation of the faults and produced further brecciation and crystallization of Group-C schorl.

istry of A-type granitoids in the Divrigi–Sivas region, eastern-central Anatolia, Turkey. *Lithos* **97**, 193-218.

BOZTUĞ, D., TICHOMIROWA, M. & BOMBACH, K. (2007a): ^{207}Pb–^{206}Pb single zircon evaporation ages of some granitoid rocks reveal continent – oceanic island arc collision during the Cretaceous geodynamic evolution of the central Anatolian crust, Turkey. *J. Asian Earth Sci.* **31**, 71-86.

CHAUSSIDON, M. & MARTY, B. (1995): Primitive boron isotope composition of the mantle. *Science* **269**, 383-386.

CLARK, C. & JAMES, P. (2003): Hydrothermal brecciation due to fluid pressure fluctuations: examples from the Olary Domain, South Australia. *Tectonophysics* **366**, 187-206.

CLARK, C.M. (2007): Tourmaline: structural formula calculations. *Can. Mineral.* **45**, 229-237.

DIRIK, K. & GÖNCÜOĞLU, M.C. (1996): Neotectonic characteristics of central Anatolia. *Int. Geol. Rev.* **38**, 807-817.

DIRIK, K., GÖNCÜOĞLU, M.C. & KOZLU, H. (1999): Stratigraphy and pre-Miocene tectonic evolution of the southwestern part of the Sivas Basin, central Anatolia, *Geol. J.* **34**, 303-319.

ERLER, A., AKIMAN, O., UNAN, C., DALKILIÇ, F., DALKILIÇ, B., GEVEN, A. & ÖNEN, P. (1991): Petrology and geochemistry of the magmatic rocks of the Kirsehir Massif at Kaman (Kirsehir) and Yozgat. *Doga, Turkish Journal of Engineering and Environmental Sciences* **15**, 76-100 (in Turkish).

GÖNCÜOĞLU, M.C. (1982): U/Pb ages of Nigde Massif paragneisses. *Geol. Soc. Turkey, Bull.* **25**, 61-66 (in Turkish).

GÖNCÜOĞLU, M.C., DIRIK, K., KELER, A. & YALINIZ, K. (1994): Geology of the eastern Central Anatolian Massif. 4. Relation with the Sivas Basin. TPAO Rep. 3535 (unpubl.).

GÖNCÜOĞLU, M.C., DIRIK, K. & KOZLU, H. (1997): General characteristics of pre-Alpine and Alpine terranes in Turkey: explanatory notes to the terrane map of Turkey. *Annales Géologiques des Pays Hélleniques* **37**, 515-536.

GÖNCÜOĞLU, M.C., ERLER, A., TOPRAK, V., YALINIZ, M.K., OLGUN, E. & ROJAY, B. (1992): Geology of the western

section of Central Anatolian Massif. 2. Central section. *TPAO Rep*. **3155** (unpubl.).

GÖNCÜOĞLU, M.C., TOPRAK, V., KUSCU, İ., ERLER, A. & OLGUN, E. (1991): Geology of the western section of Central Anatolian Massif. 1. Southern section. *TPAO Rep*. **2909** (unpubl.).

GÖNCÜOĞLU, M.C., TURHAN, N., SENTÜRK, K., ÖZCAN, A., UYSAL, S. & YALINIZ, M.K. (2000): A geotraverse across northwestern Turkey: tectonic units of the Sakarya region and their tectonic evolution. *In* Tectonics and Magmatism in Turkey and the Surrounding Area (E. Bozkurt, J.A. Winchester & J.D.A. Piper, eds.). *Geol. Soc., Spec. Publ.* **173**, 139-161.

GÖNCÜOĞLU, M.C. & TÜRELI, T.K. (1993): Petrology and geodynamic interpretation of plagiogranites from Central Anatolian ophiolites. *Turkish J. Earth Sci*. **2**, 195-203.

GRICE, J.D. & ROBINSON, G.W. (1989): Feruvite, a new member of the tourmaline group, and its crystal structure. *Can. Mineral*. **27**, 199-203.

GUILLOU-FROTTIER, L. & BUROV, E. (2003): The development and fracturing of plutonic apexes: implications for porphyry ore deposits. *Earth Planet. Sci. Lett*. **214**, 341-356.

HAWTHORNE, F.C. & HENRY, D.J. (1999): Classification of the minerals of the tourmaline group. *Eur. J. Mineral*. **11**, 201-215.

HELGESON, H.C. (1992). Effects of complex formation in flowing fluids on the hydrothermal solubilities of minerals as a function of fluid pressure and temperature in the critical and supercritical regions of the system H_2O. *Geochim. Cosmochim. Acta* **56**, 3191-3207.

HENRY, D.J. & DUTROW, B.L. (1992): Tourmaline in a low grade clastic metasedimentary rocks: an example of the petrogenetic potential of tourmaline. *Contrib. Mineral. Petrol*. **112**, 203-218.

HENRY, D.J. & DUTROW, B.L. (1996): Metamorphic tourmaline and its petrologic applications. *In* Boron: Mineralogy, Petrology, and Geochemistry (E.S. Grew & L.M. Anovitz, eds.). *Rev. Mineral*. **33**, 503-557.

HENRY, D.J. & GUIDOTTI, C.V. (1985). Tourmaline as a petrogenetic indicator mineral: an example from the staurolite-grade metapelites of NW Maine. *Am. Mineral*. **70**, 1-15.

ILBEYLI, N., PEARCE, J.A., THIRLWALL, M.F. & MITCHELL, J.G. (2004): Petrogenesis of collision-related plutonics in Central Anatolia, Turkey. *Lithos* **72**, 163-182.

ISIK, V., LO, CHING-HUA, GÖNCÜOGLU, M.C. & DEMIREL, S. (2008): $^{40}Ar/^{39}Ar$ ages from the Yozgat Batholith: preliminary data on the timing of Late Cretaceous extension in the Central Anatolian Crystalline Complex, Turkey. *J. Geol*. **116**, 510-526.

JIANG, SHAO-YONG, PALMER, M.R., MCDONALD, A.M., SLACK, J.F. & LEITCH, C.H.B. (1996): Feruvite from the Sullivan Pb–Zn–Ag deposit, British Columbia. *Can. Mineral*. **34**, 733-740.

KADIOGLU, Y.K. & GÜLEC, N. (1999): Types and genesis of the enclaves in Central Anatolian granitoids. *Geol. J*. **34**, 243-256.

KÖKSAL, S., ROMER, R.L., GÖNCÜOGLU, M. & TOKSOY-KÖKSAL, F. (2004): Timing of post-collisional H-type to A-type granitic magmatism: U–Pb titanite ages from the Alpine central Anatolian granitoids (Turkey). *Int. J. Earth Sci*. **93**, 974-989.

LONDON, D. & MANNING, D.A.C. (1995): Chemical variation and significance of tourmaline from southwest England. *Econ. Geol*. **90**, 495-519.

LONDON, D., MORGAN, G.B., VI & HERVIG, R.L. (1989): Vapor-undersaturated experiments with Macusani glass + H_2O at 200 MPa, and the internal differentiation of granitic pegmatites. *Contrib. Mineral. Petrol*. **102**, 1-17.

LORILLEUX, G., JÉBRAK, M., CUNEY, M. & BAUDEMONT, D. (2002): Polyphase hydrothermal breccias associated with unconformity-related uranium mineralisation (Canada): from fractal analysis to structural significance. *J. Struct. Geol*. **24**, 323-338.

MARSCHALL, H.R., LUDWIG, T., ALTHERR, R., KALT, A. & TONARINI, S. (2006): Syros metasomatic tourmaline: evidence for very high-$\delta^{11}B$ fluids in subduction zones. *J. Petrol*. **47**, 1915-1942.

MCDONOUGH, W.F. & SUN, S.S. (1995): The composition of the Earth. *Chem. Geol*. **120**, 223-253.

NORTON, D.L. & DUTROW, B.L. (2001): Complex behavior of magma–hydrothermal processes: role of supercritical fluid. *Geochim. Cosmochim. Acta* **65**, 4009-4017.

POUCHOU, J.L. & PICHOIR, F. (1985): "PAP" $\phi(\rho Z)$ correction procedure for improved quantitative microanalysis. *In* Microbeam Analysis (J.T. Armstrong, ed.). San Francisco Press, San Francisco, California (104-106).

RIDLEY, J. (1993): The relations between mean rock stress and fluid flow in the crust, with reference to vein- and lode-style gold deposits. *Ore Geol. Rev.* **8**, 23-37.

RYAN, J.G. & LANGMUIR, C.H. (1993): The systematics of boron abundances in young volcanic rocks. *Geochim. Cosmochim. Acta* **57**, 1489-1498.

SENGÖR, A.M.C. & YILMAZ, Y. (1981): Tethyan evolution of Turkey: a plate tectonic approach. *Tectonophysics* **75**, 181-241.

SEYMEN, Ü. (1981): Stratigraphy and metamorphism of Kırsehir Massif in the vicinity of Kaman (Kırşehir). *Geol. Soc. Turkey Bull*. **24**, 101-108 (in Turkish).

SHINOHARA, H., KAZAHAYA, K. & LOWENSTERN, J.B. (1995): Volatile transport in a convecting magma column: impli-

cations for porphyry Mo mineralization. *Geology* **23**, 1091-1094.

SILLITOE, R.H. & SAWKINS, F.J. (1971): Geologic, mineralogic and fluid inclusion studies relating to the origin of the copper-bearing tourmaline-breccia pipes, Chile. *Econ. Geol.* **66**, 1028-1041.

SKEWES, M.A., HOLMGREN, C. & STERN, C.R. (2003): The Donoso copper-rich tourmaline-bearing breccia pipe in central Chile: petrologic, fluid inclusion and stable isotope evidence for an origin from magmatic fluids. *Mineral. Deposita* **38**, 2-21.

SLACK, J.F., HERRIMAN, N., BARNES, R.G. & PLIMER, I.R. (1984): Stratiform tourmalinites in metamorphic terranes and their geologic significance. *Geology* **12**, 713-716.

TAYLOR, S. R. & MCLENNAN, S. M. (1985): *The Continental Crust: Its Composition and Evolution*. Blackwell, Oxford, U.K.

TITLEY, S.R. & BEANE, R.E. (1981): Porphyry copper deposits. I. Geologic settings, petrology and tectonogenesis. *Econ. Geol., 75th Anniv. Vol.*, 214-235.

TRUMBULL, R.B. & CHAUSSIDON, M. (1999): Chemical and boron isotopic composition of magmatic and hydrothermal tourmalines from the Sinceni granite–pegmatite system in Swaziland. *Chem. Geol.* **153**, 125-137.

WARNAARS, F.W., HOLMGREN, C. & BARASSI, S. (1985): Porphyry copper and tourmaline-breccias at Los Bronces – Rio Blanco, Chile. *Econ. Geol.* **80**, 1544-1565.

WEISBROD, A., POLAK, C. & ROY, D. (1986): Experimental study of tourmaline solubility in the system Na–Mg–Al–Si–B–O–H: applications to the boron content of natural hydrothermal fluids and tourmalinization processes. *Int. Symp. Experimental Mineral., Abstr.* **1**, 140-141 (abstr.).

WHITNEY, D.L. & DILEK, Y. (2001): Metamorphic and tectonic evolution of the Hırkadag Block, Central Anatolian Crystalline Complex. *Turkish J. Earth Sci.* **10**, 1-15.

WHITNEY, D.L. & HAMILTON, M.A. (2004): Timing of high-grade metamorphism in central Turkey and the assembly of Anatolia. *J. Geol. Soc. London* **161**, 823-828.

WILLIAMSON, B.J., SPRATT, J., ADAMS, J.T. & STANLEY, C.J. (2000): Geochemical constraints from zoned hydrothermal tourmalines on fluid evolution and Sn mineralization: an example from Fault Breccias at Roche, SW England. *J. Petrol.* **41**, 1439-1453.

YALINIZ, K. & GÖNCÜOĞLU, M.C. (1999): Clinopyroxene compositions of the isotropic gabbros from the Sarıkaraman ophiolite: new evidence on supra-subduction zone type magma genesis in central Anatolia. *Turkish J. Earth Sci.* **8**, 103-111.

Received November 21, 2008, revised manuscript accepted July 22, 2009.